Supporting Information

Enhanced Supply of Hydroxyl Species in CeO_2-Modified Platinum Catalyst Studied by *in situ* ATR-FTIR Spectroscopy

*Yu Katayama, Takeou Okanishi, Hiroki Muroyama, Toshiaki Matsui, Koichi Eguchi**

Department of Energy and Hydrocarbon Chemistry, Graduate School of Engineering, Kyoto University, Kyoto 615-8510, Japan

Corresponding Author

*Corresponding author. Tel.: +81-75-383-2519; fax: +81-75-383-2520

E-mail address: eguchi@scl.kyoto-u.ac.jp (K. Eguchi)

Effect of ionomer on the electrochemical and IR responses

Figure S1 shows the cyclic voltammograms of a bare Pt/Si prism and ionomer-coated Pt/Si prisms collected with the prisms in the spectro-electrochemical cell. The shape of the voltammogram for the ionomer-coated Pt/Si prism was similar to that of the bare Pt/Si prism, indicating that the effect of the ionomer coating on the electrochemical response was negligible.

Figure S2 shows the representative time-resolved ATR-FTIR spectra of the bare Pt surface simultaneously acquired with the linear sweep voltammogram in 1 M KOH. The response of the OH_{ad} band, observed at 1616 cm^{-1}, over the bare Pt surface was almost identical to that of the ionomer-coated Pt surface (Figure 5 in the manuscript). This result suggested that the IR response was also unaffected by the presence of the ionomer.

The electrochemical surface areas (ECSAs) of various electrodes used in this study are summarized in Table S1. For the Pt disk electrode, the ionomer coating and CeO_2 modification led to a slight reduction in ECSA. Notably, in the case of the Pt/Si prisms, the same comparison could not be conducted because each prism was prepared separately. In addition, we noted that the ECSA did not change even after electrochemical measurements such as CV and CA, indicating that the ECSA was substantially the same throughout the experiment.

Effect of deuterium substitution on the 1130 cm^{-1} band

Figures S3 (a) and (b) show *in situ* ATR-FTIR spectra of the ionomer-coated Pt surface simultaneously acquired with linear sweep voltammograms in 1 M KOH and 1 M KOD. The KOD solution used for this experiment was prepared from 40 wt% KOD in D_2O (Aldrich, 98 atom% D) and D_2O (Aldrich, 99.9 atom% D). In the case of 1 M KOD, the peak position of the vibration mode originating from the hydrogen-containing chemicals should show a substantial shift in wavenumber because of the isotopic exchange. In Figure S3 (a), a clear peak emerged at 1130 cm^{-1} at potentials greater than 0.7 V; this peak was assigned to the librational mode of OH_{ad} species adsorbed onto the Pt surface. In contrast, in the case of the deuterium-substituted condition (Figure S3 (b)), no band was observed at *ca*. 1130 cm^{-1}, where the librational mode of Pt-OH_{ad} species was observed in 1 M KOH. The disappearance of this band is explained by isotopic exchange. Thus, this observation supports the hypothesis that the band at 1130 cm^{-1} originates from OH_{ad} species. Note that, in the case of 1 M KOD, a negative-going band was observed at *ca*. 1180 cm^{-1}, which matches well with the reported wavenumber of the interfacial D_2O band[1 2 3]. Figure S3 (c) shows IR spectra of the CeO_2-modified Pt surface in 1 M KOH. As with the result shown in Figure S3 (a), the Pt–OH_{ad} band at 1130 cm^{-1} was also confirmed, with no shift in wavenumber after CeO_2 modification. However, in the case of the CeO_2-modified Pt surface, the Pt–OH_{ad} band started to emerge at distinctively low potentials, approximately 0.3 V, indicating the effect of the CeO_2 additive on the OH adsorption behavior.

Potential dependence of peak wavenumber for the Pt–OH_{ad} band

Figure S4 shows the potential dependency of the peak wavenumber for the Pt–OH_{ad} band of both the ionomer-coated and CeO_2-modified Pt/Si prisms. Note that the shift of the peak wavenumber was mainly caused by dipole–dipole interactions between the adsorbed species, which strongly depended upon the amount of surface adsorbed species[4]. Therefore, the amount of peak shift for the Pt–OH_{ad} band also reflects the amount of OH_{ad} species on the Pt surface. A comparison of the results obtained in 1 M KOH reveals that the Pt–OH_{ad} band shift started at an earlier potential for the CeO_2-modified Pt surface than for the ionomer-coated Pt surface. This result suggests that the adsorption of OH onto Pt was accelerated by CeO_2 modification. However, the overall band shift was almost the same for both Pt surfaces, indicating that the total amount of OH_{ad} species, that is, the OH_{ad} coverage of Pt, was only slightly affected by surface modification[4]. Moreover, it is important to note that in the presence of NH_3, the amount of band shift became smaller than that in the presence of 1 M KOH. This behavior is partially due to the consumption of OH_{ad} species during the ammonia oxidation reaction. In the case of the ionomer-coated Pt surface, the Pt–OH_{ad} band shift began at *ca*. 0.8 V, which is 0.2 V higher than that of the Pt surface in 1 M KOH. This result clearly indicates that the OH_{ad} species was in short supply for the ionomer-coated Pt surface, resulting in inhibition of OH adsorption at potentials between 0.6 V and 0.8 V, where the ammonia oxidation reaction was still in progress. In contrast, because of the enhancement of the OH_{ad} supply by CeO_2 modification, a sufficient supply of OH_{ad} was available

even during the ammonia oxidation reaction, which led to the shift in the Pt–OH_{ad} band in CeO_2-modified Pt in the potential range from 0.2 to 1.2 V. In summary, the potential dependency of the peak wavenumber for the Pt–OH_{ad} band was consistent with the potential dependency of the Pt–OH_{ad} band area shown in Figures 7 and 11.

Difference in potential dependencies of the band area of interfacial water

Figure S5 shows the potential dependency of the band area at 1616 cm^{-1}, which is related to the interfacial water, for both the ionomer-coated and CeO_2-modified Pt surfaces in 1 M KOH. We defined the H_2O_{ad} band area as the absolute value of the integration of absorbance for the 1616 cm^{-1} band. The potential dependency of the calculated H_2O_{ad} band area for the Pt surface was approximately related to the CV response, which strongly indicated the effect of surface-adsorbed species on interfacial H_2O_{ad} (Figure S5 (a)). Given that the result was obtained in 1 M KOH, the interfacial H_2O_{ad} was partially replaced by other absorbed species (likely OH_{ad}) under polarization. Interestingly, in the case of the CeO_2-modified Pt/Si prism, the tendency was different. As shown in Figure S5 (b), the H_2O_{ad} band area simply responded linearly to the applied potential. As mentioned in the text, in the case of CeO_2-modified Pt, the OH_{ad} species is adsorbed not only onto the Pt surface but also onto the CeO_2 additive. Therefore, this change in the potential dependency of the H_2O_{ad} band area is mainly due to the interaction between H_2O_{ad} and OH_{ad} species adsorbed onto the CeO_2 surface.

Time dependency of the band area during potentiostatic operation

To ensure the validity of the peculiar change in adsorption property observed during LSV, we conducted *in situ* ATR-FTIR measurements during the potentiostatic operation at 0.6 V, where the NH_3 oxidation proceeded. The focus was centered on the following two species: the $N_2H_{4,ad}$ species, which was a reaction intermediate, and the NO_{ad} species, which was affected by the amount of OH_{ad} species supplied to the Pt active sites. Figure S6 shows the time course of the band area of these species in both the ionomer-coated Pt/Si prism and the CeO_2-modified Pt/Si prism. The band area was calculated and normalized in the same manner as that in Figure 11, and the band area at 0 s (before potentiostatic operation) was set to zero. The band area of the $N_2H_{4,ad}$ species rapidly increased soon after the beginning of potentiostatic operation, but the initial growth of the band area in the CeO_2-modified Pt/Si prism was much larger. This behavior agrees well with the chronoamperometric responses. For the highly active catalyst (in this case, the CeO_2-modified Pt/Si prism), more $NH_{3,ad}$ species were dehydrogenated to $NH_{x,ad}$ species and promoted the dimerization to form $N_2H_{4,ad}$ species, which resulted in a larger band area of $N_2H_{4,ad}$ species. After this abrupt growth in $N_2H_{4,ad}$ band area, the band area gradually decayed in the spectra of both prisms because the number of active Pt sites where the dehydrogenation of $NH_{x,ad}$ proceeded was decreased, probably because of surface poisoning. The two prisms showed almost the same time dependency for NO_{ad} species, but the value of the band area was much larger in the case of the CeO_2-modified Pt/Si prism. As described in the article, this

increase in the band area should be related to the enhancement of OH adsorption by the CeO_2 additive. Because the band area slightly increased with time, the NO_{ad} species should occupy a portion of Pt surface sites, resulting in a decrease in the number of active sites. In either case, the increase in both $N_2H_{4,ad}$ and NO_{ad} band areas was observed in the case of the CeO_2-modified catalyst, consistent with the results obtained during LSVs.

Linear sweep voltammograms used for calculations in Figure 12

First, the stability of the CeO_2 additive was reconfirmed by measuring the cyclic voltammograms in 1 M $HClO_4$. As shown in Figure S7, no change was observed in the voltammogram waveform, indicating that CeO_2 stably existed under these conditions. Figures S8–S11 show the linear sweep voltammograms measured in the presence of 0.1 M NH_3, 1 M ethanol, 1 M methanol, and CO. All the current densities expressed were normalized by ECSA. The vertical line shown in each figure indicates the potential where the peak current density was used for the calculation of Figure 12. The actual value of peak current density is also provided in parentheses. Note that the onset potential of each reaction hardly affected by the CeO_2 modification.

References

1. Max, J. J.; Chapados, C., *J. Chem. Phys.,* **2009,** *131*, 184505.

2. Lappi, S. E.; Smith, B.; Franzen, S., *Spectrochim. Acta A,* **2004,** *60*, 2611-2619.

3. Kunimatsu, K.; Senzaki, T.; Samjeské, G.; Tsushima, M.; Osawa, M., *Electrochim. Acta,* **2007,** *52*, 5715-5724.

4. Persson, B. N. J.; Ryberg, R., *Phys. Rev. B,* **1981,** *24*, 6954-6970.

Table S1 Electrochemical surface area (ECSA) of various electrodes used in this study

	Bare	**Ionomer coated**	**CeO_2-modified**
Pt disk	2.99 cm^2	2.98 cm^2	2.94 cm^2
Pt/Si prism	15.20 cm^2	11.75 cm^2	17.26 cm^2

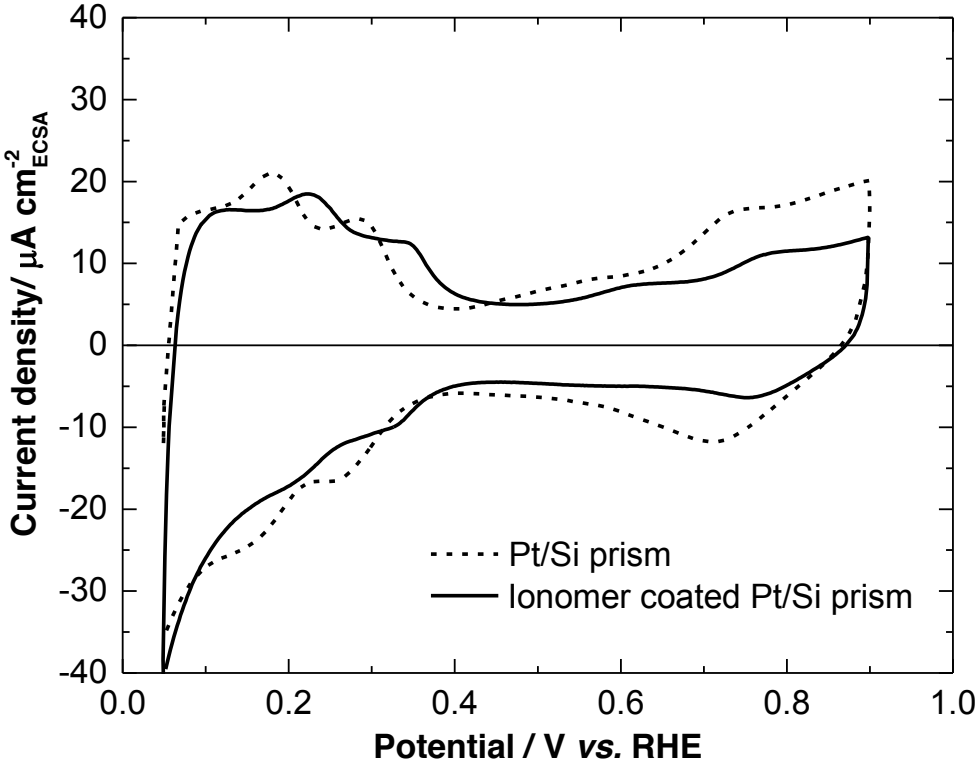

Figure S1 Cyclic voltammograms of Pt/Si prism (dotted line) and ionomer coated Pt/Si prism (solid black line) in 1 M KOH at 25ºC with a scanning rate of 20 mV s^{-1}.

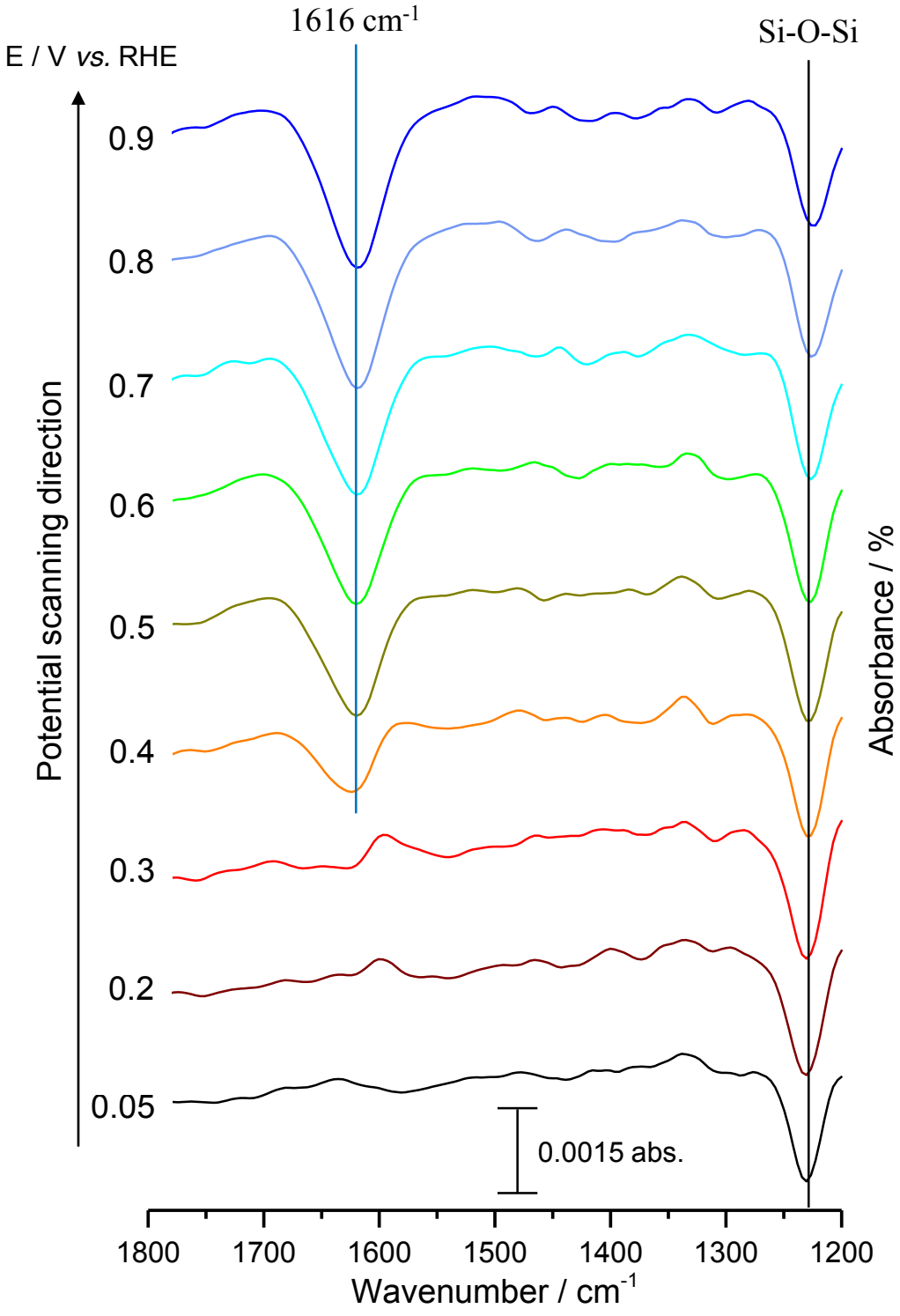

Figure S2 Time-resolved IR spectra of the Pt surface acquired simultaneously with the linear sweep voltammogram in 1 M KOH at 25ºC with a scanning rate of 20 mV s^{-1}.

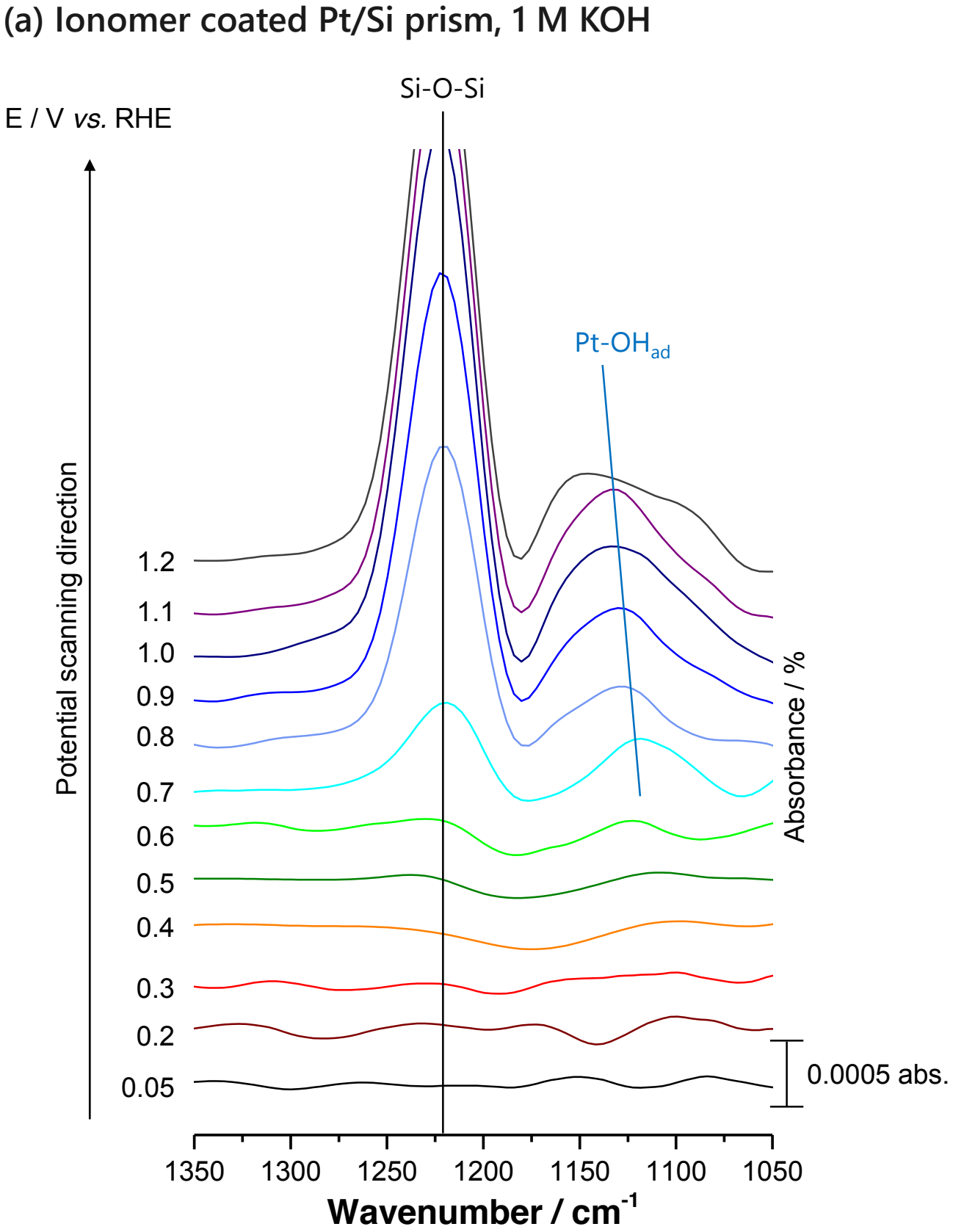

Figure S3 Time-resolved IR spectra of the (a), (b) ionomer coated and (c) CeO_2-modified Pt surface acquired simultaneously with the linear sweep voltammogram in (a), (c) 1 M KOH and (b) 1 M KOD at 25ºC with a scanning rate of 20 mV s^{-1}.

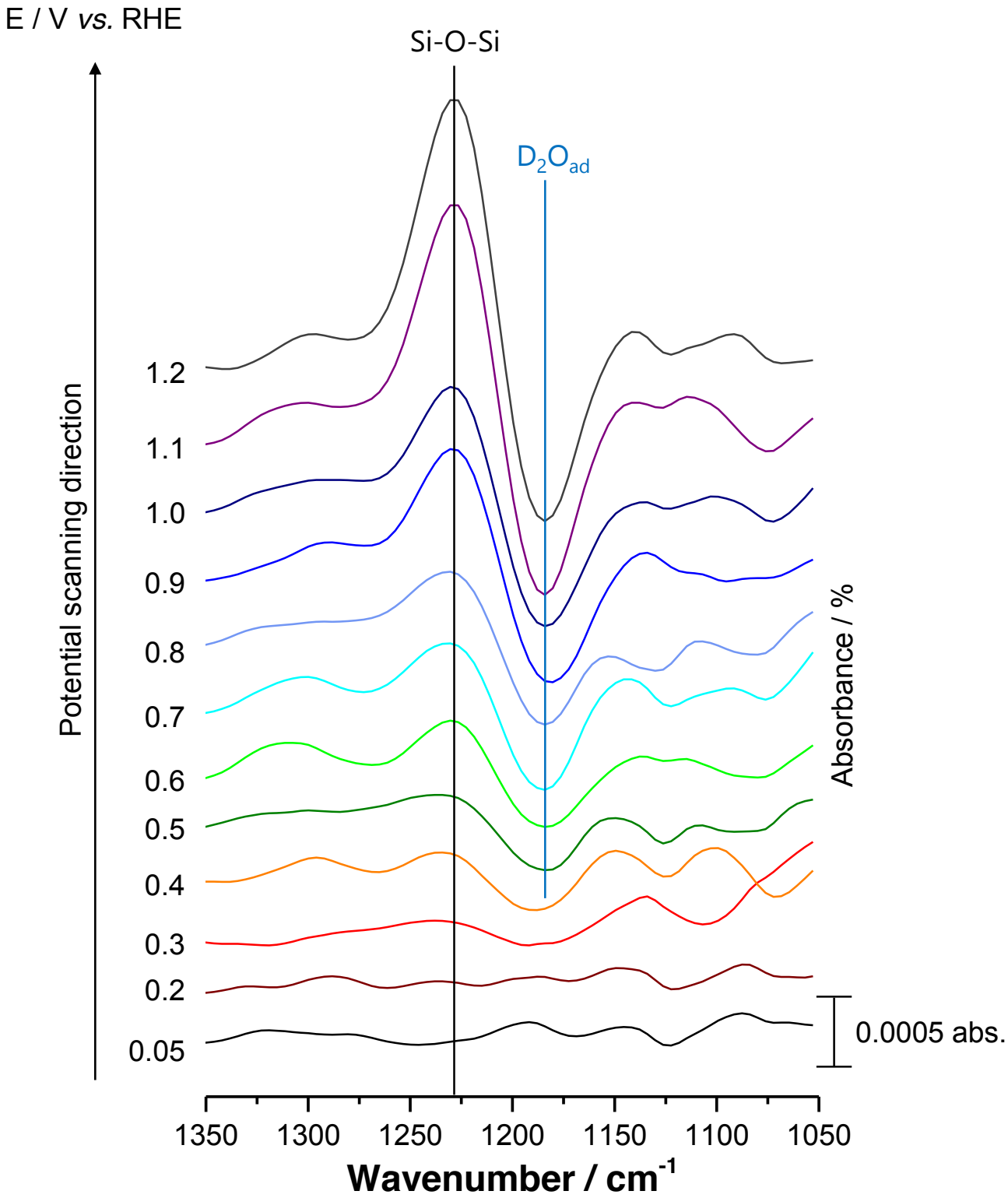

Figure S3 Time-resolved IR spectra of the (a), (b) ionomer coated and (c) CeO_2-modified Pt surface acquired simultaneously with the linear sweep voltammogram in (a), (c) 1 M KOH and (b) 1 M KOD at 25ºC with a scanning rate of 20 mV s^{-1}.

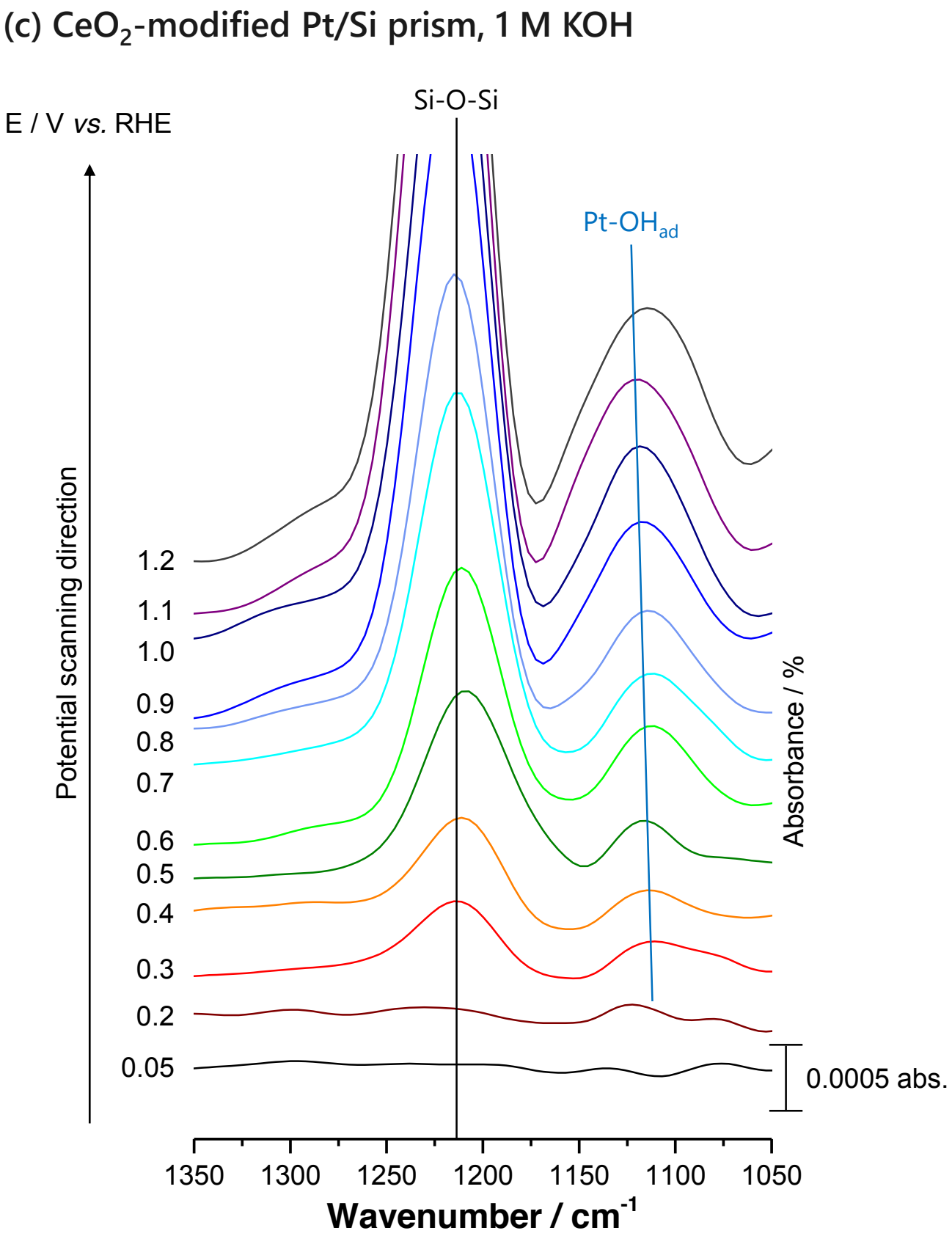

Figure S3 Time-resolved IR spectra of the (a), (b) ionomer coated and (c) CeO_2-modified Pt surface acquired simultaneously with the linear sweep voltammogram in (a), (c) 1 M KOH and (b) 1 M KOD at 25ºC with a scanning rate of 20 mV s^{-1}.

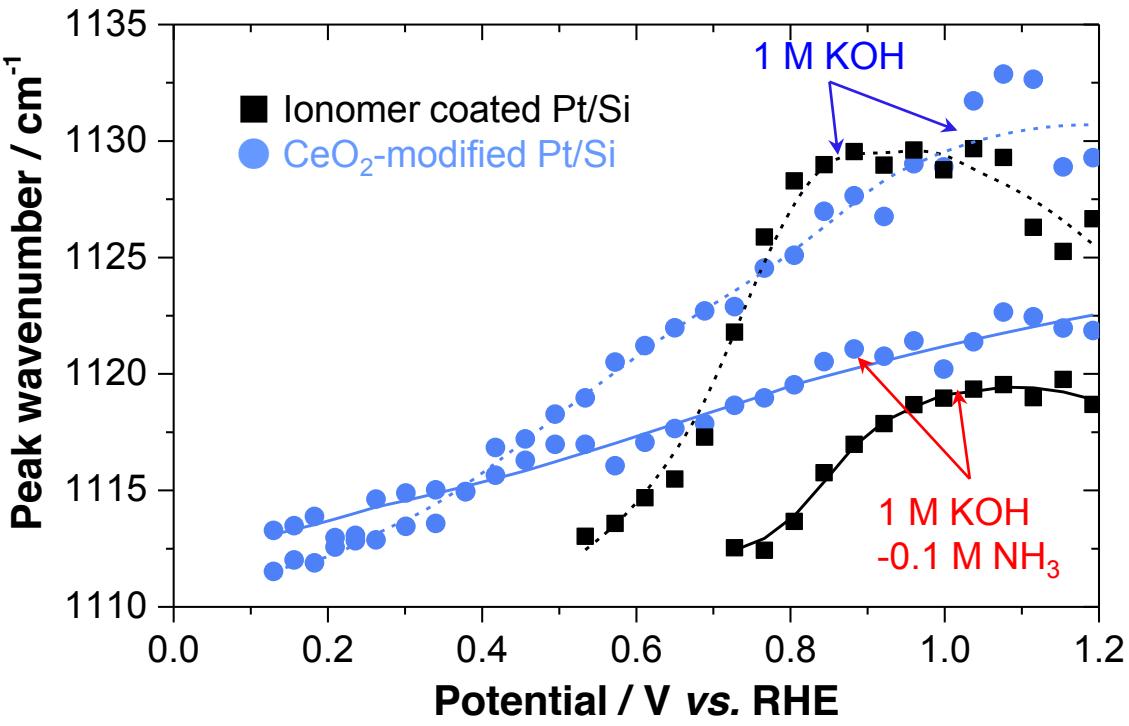

Figure S4 Potential dependency of the peak wavenumber for Pt-OH_{ad} band of ionomer coated Pt and CeO_2-modified Pt surface in 1 M KOH (broken line) and 1 M KOH–0.1 M NH_3 (solid line).

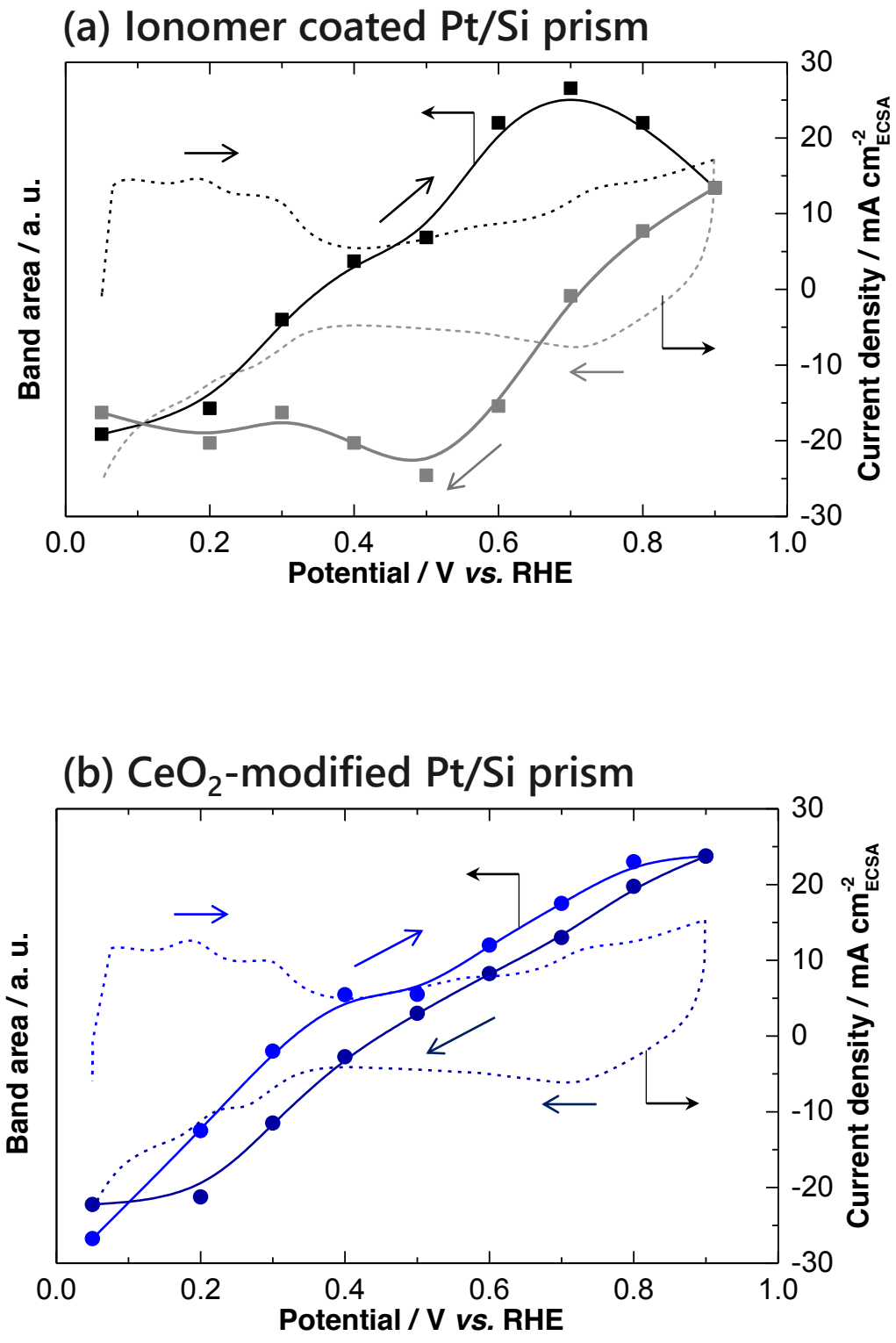

Figure S5 Potential dependency of the band area at 1616 cm^{-1} for (a) ionomer coated Pt/Si prism and (b) CeO_2-modified Pt/Si prism in 1 M KOH. Data were taken from time-resolved IR spectra acquired simultaneously with the cyclic voltamogram shown in broken line.

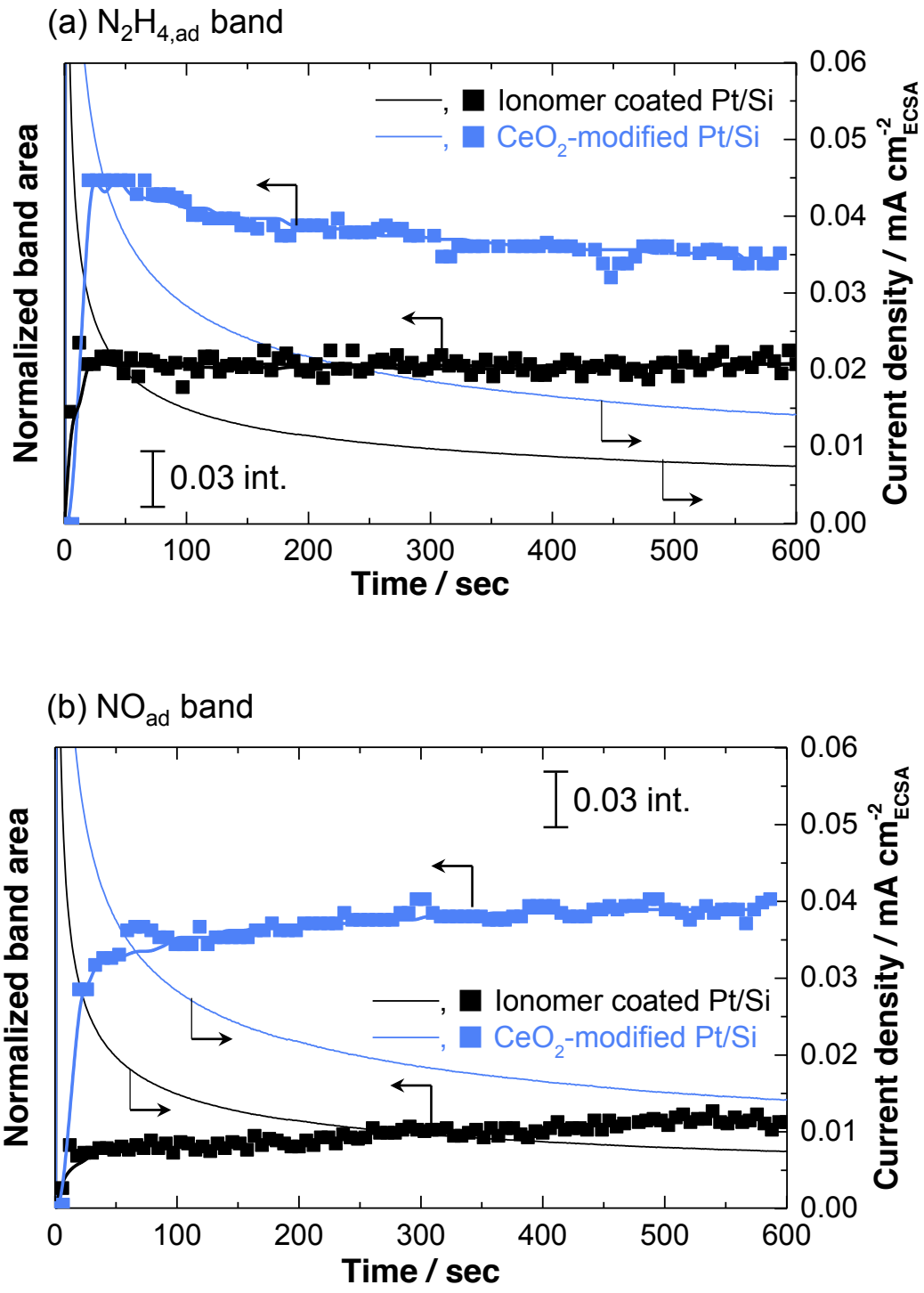

Figure S6 Time course of current density of ionomer coated Pt/Si and CeO_2-modified Pt/Si prisms and the normalized band area of (a) $N_2H_{4,ad}$ and (b) NO_{ad} at the constant potential of +0.6 V (*vs*. RHE) in 1 M KOH–0.1 M NH_3 at room temperature.

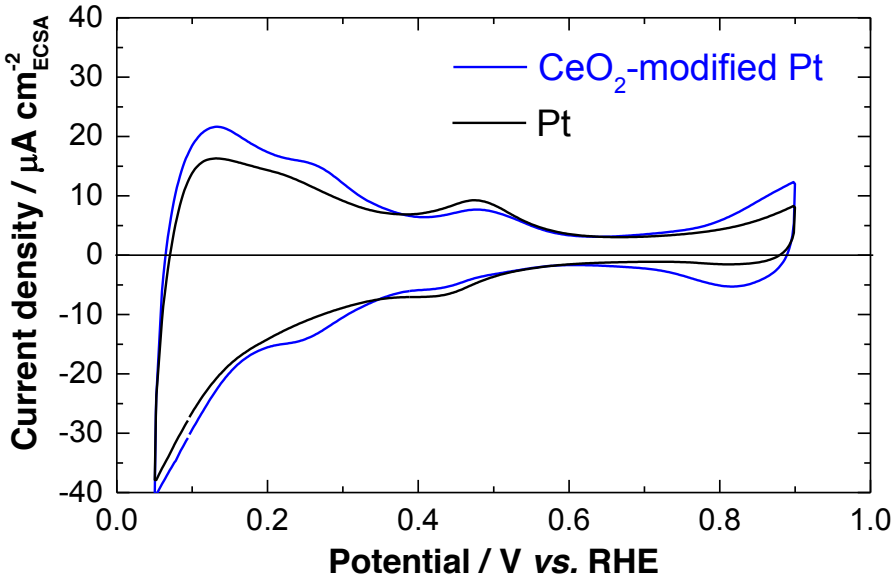

Figure S7 Cyclic voltammograms of Pt disk and CeO_2-modified Pt disk electrodes in 1 M $HClO_4$ at 25ºC with a scanning rate of 20 mV s^{-1}.

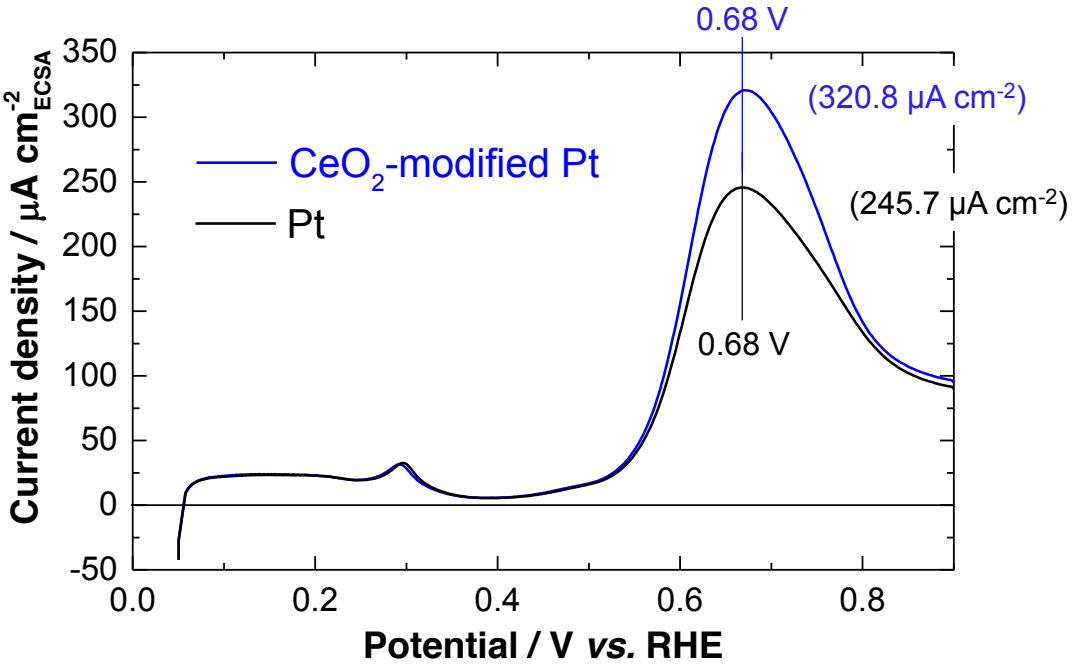

Figure S8 Linear sweep voltammograms of Pt disk and CeO_2-modified Pt disk electrodes in 1 M KOH–0.1 M NH_3 at 25ºC with a scanning rate of 20 mV s^{-1}. The actual value of peak current density was provided in parentheses.

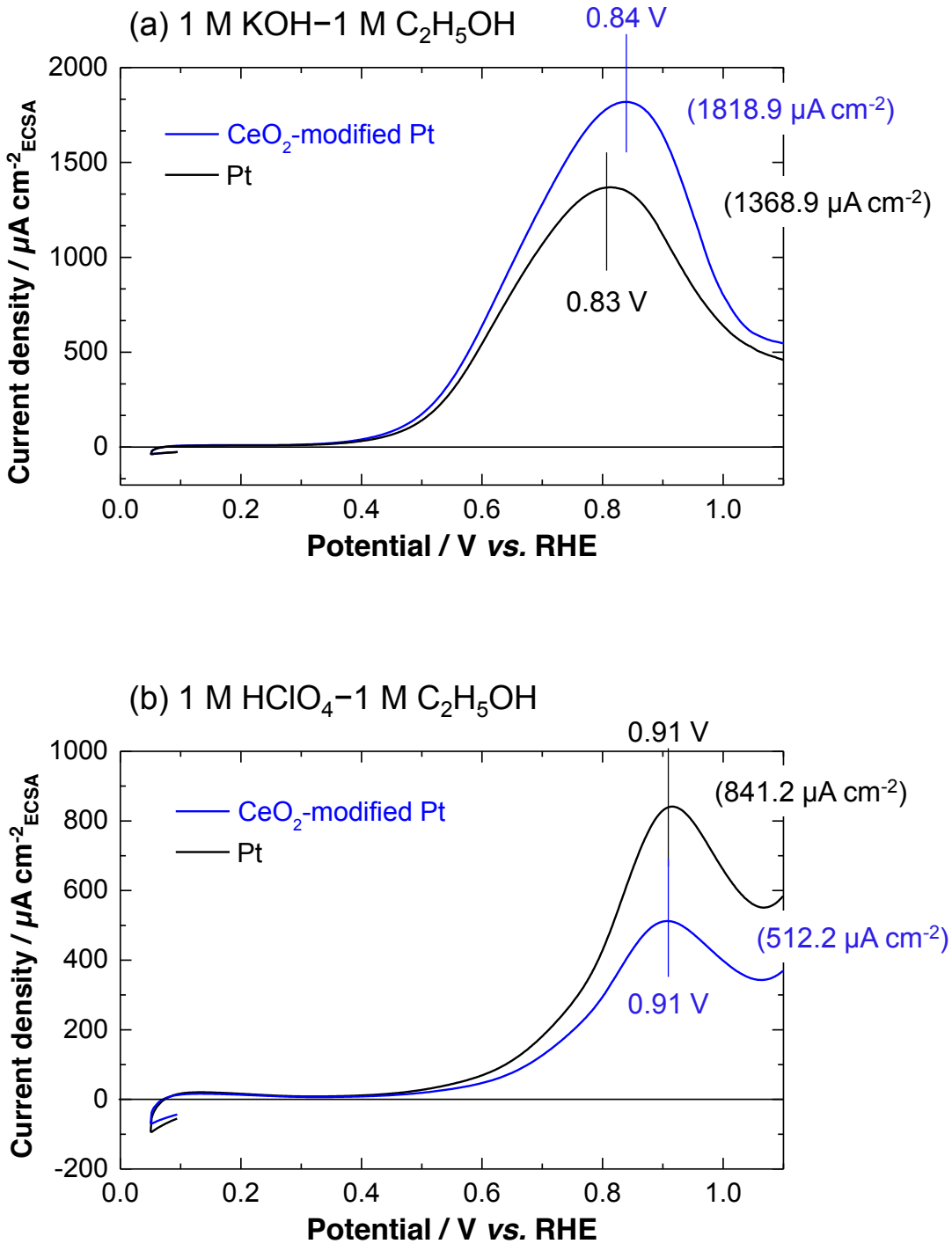

Figure S9 Linear sweep voltammograms of Pt disk and CeO_2-modified Pt disk electrodes in (a) 1 M KOH–1 M C_2H_5OH and (b) 1 M $HClO_4$–1 M C_2H_5OH at 25ºC with a scanning rate of 20 mV s^{-1}. The actual value of peak current density was provided in parentheses.

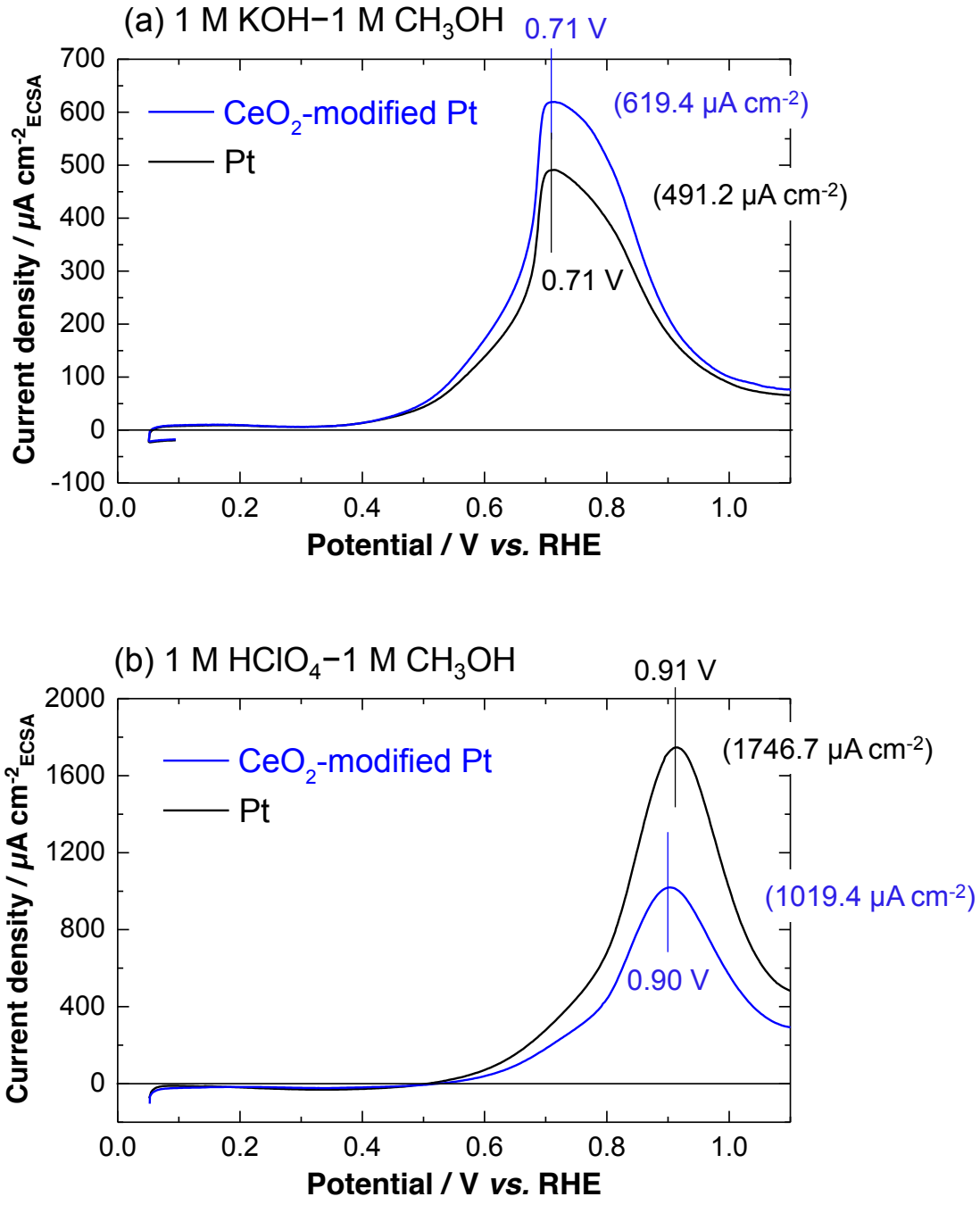

Figure S10 Linear sweep voltammograms of Pt disk and CeO_2-modified Pt disk electrodes in (a) 1 M KOH–1 M CH_3OH and (b) 1 M $HClO_4$–1 M CH_3OH at 25ºC with a scanning rate of 20 mV s^{-1}. The actual value of peak current density was provided in parentheses.

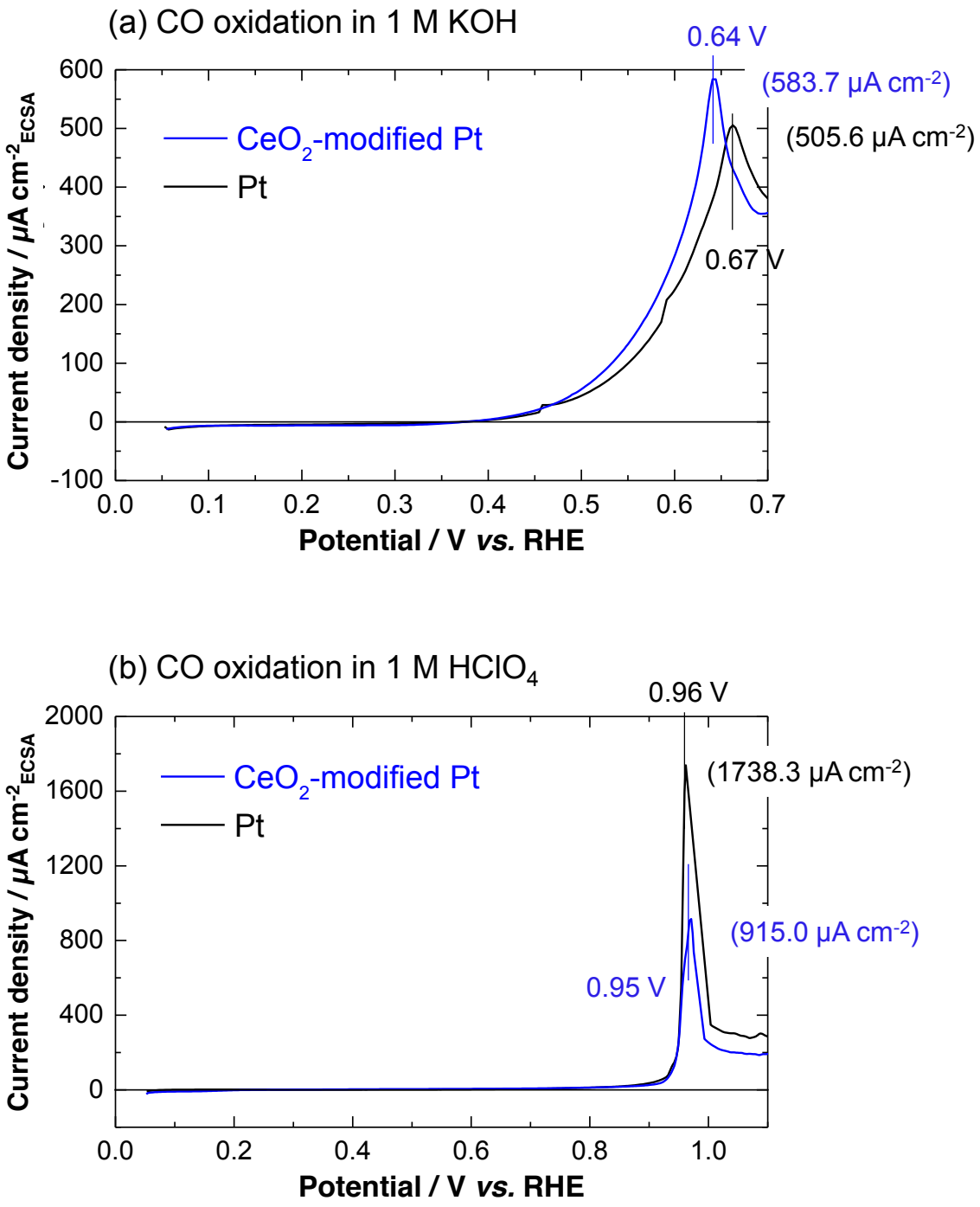

Figure S11 Linear sweep voltammograms of Pt disk and CeO_2-modified Pt disk electrodes in the presence of CO in (a) 1 M KOH and (b) 1 M $HClO_4$ at 25ºC with a scanning rate of 20 mV s^{-1}. The actual value of peak current density was provided in parentheses.